SUPPLEMENTARY INFORMATION

Phase Engineering of 2D X2C Monolayers: Insights into Metal-Semiconductor Transitions and Multifunctional Applications

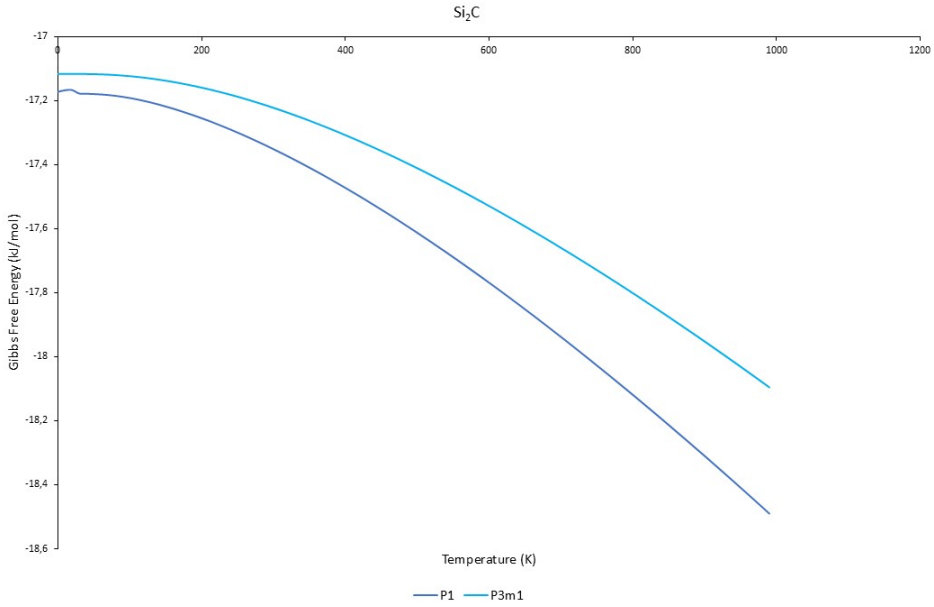

Figure S1. Gibbs free energy vs Temperature for Si_2C in the P1 (blue) and P3m1 (cyan) phases.

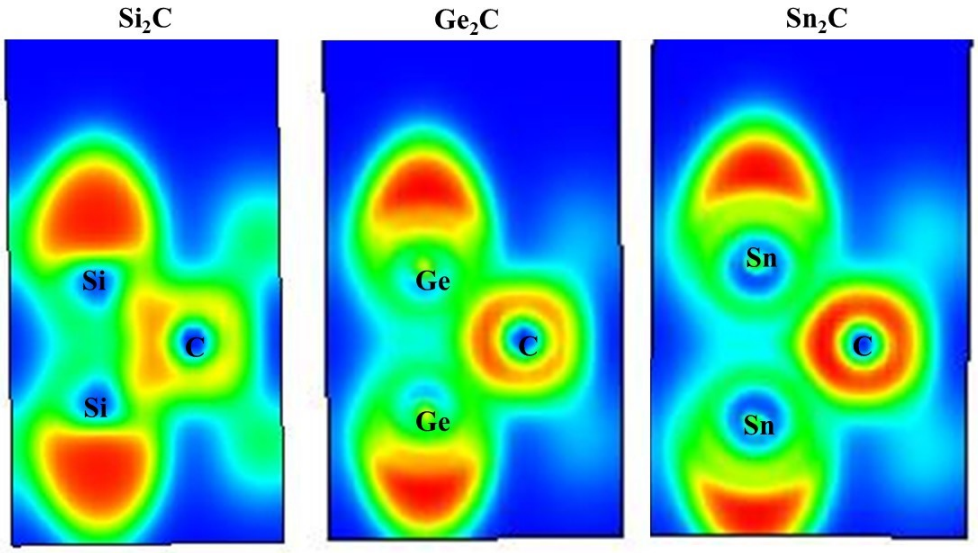

Figure S2. 2D electron localization function (ELF) of the X_2C structures in the P3m1 phase.

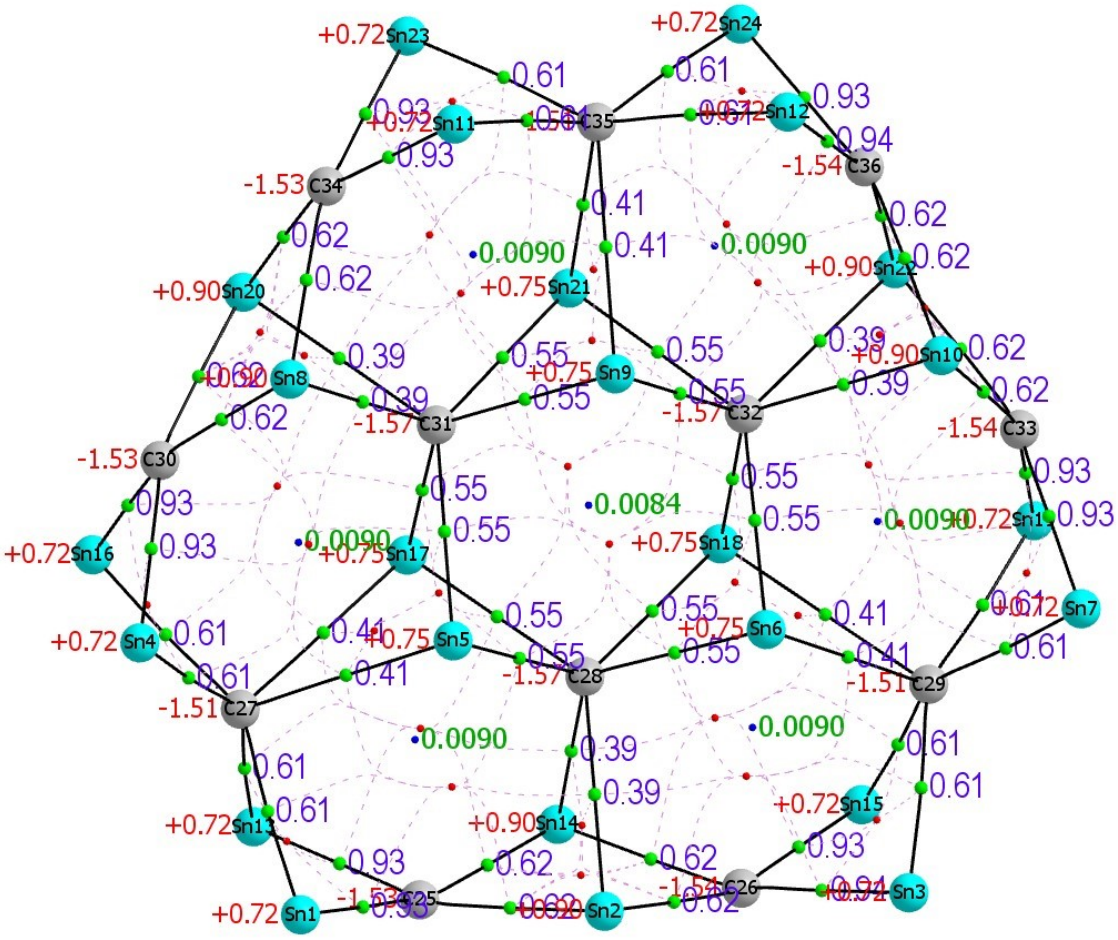

Figure S3. Quantum Theory of Atoms in Molecules (QTAIM) analysis in Sn_2C cluster model. C and Sn atoms are shown in grey and cyan, respectively.

In Figure S3, the nuclei (Sn atoms in cyan and C atoms in grey) are connected by the bond paths (black lines) representing the sequence of maxima in electron density between two nuclei. Each bond path has his lowest point of electron density, the Bond Critical Point (BCP), represented as a green ball. In blue are shown the values of Delocalization Indices (DI), which are associated with the classical bond order. The red balls indicate the Ring Critical Points (RCP), which are the points on the ring surfaces with the lowest electron density. Dashed lines connect each BCP to the central RCP. As a 3D structure, the supercell forms cages delimited by the pseudo-rings established by a series of nuclei. Thus, each cage has a lowest electron density point, which is depicted by blue balls. In these Cage critical points (CCP) the electron density values are shown in green (values that are almost insignificant).

For Sn_2C, the electron density distribution in the supercell is higher between a C nucleus and two Sn nuclei, reaching a DI value of 0.93-0.94, which can be associated to a single bond and shows two additional interactions with a DI value of 0.61-0.62. This is observed when a C atom is located in one of the three lateral faces. When the C atom is one of the three atoms located in a truncated corner, i.e. those that have 6 contacts with Sn, the DI values are 0.61 for the surface bonds and 0.41 for the internal bonds. The three internal C atoms also exhibit 6 contacts; the DI values being 0.55 and 0.39 (for the radial bonds). Thus, the bonding organization and the amount of electron density shared by each C atom depends on the position in the supercell, i.e. the number of Sn atoms contacted. In this case, the center of the Sn_2C cluster is a good representation of the periodic model.

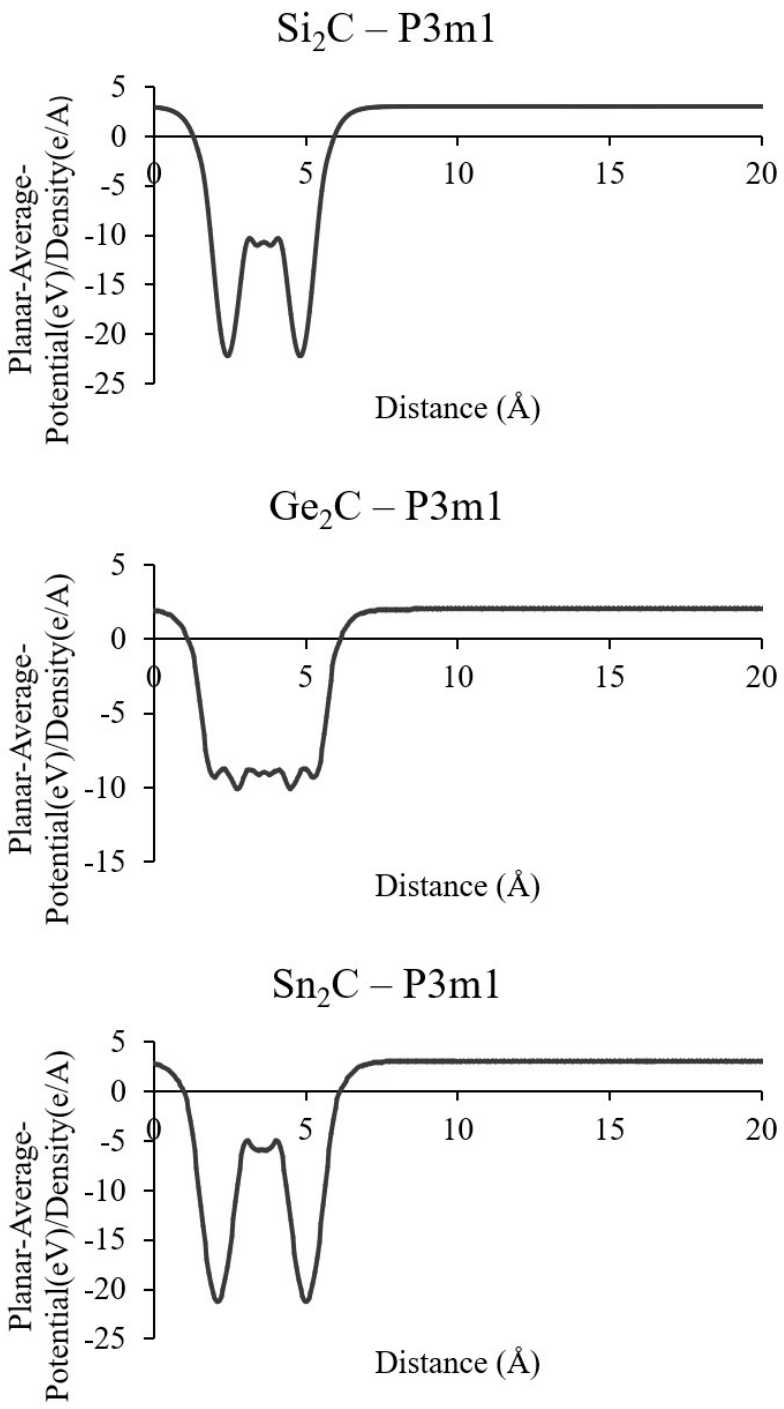

Figure S4. Potential vs. distance function for the polar (P3m1 phase) Si_2C, Ge_2C and Sn_2C monolayers.

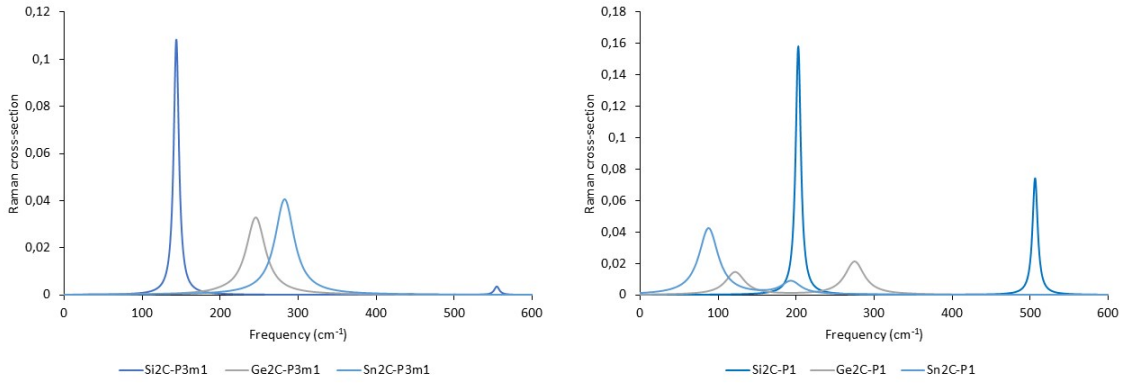

Figure S5. Raman spectra of Si_2C, Ge_2C and Sn_2C monolayers in the P3m1 and P1 phases.

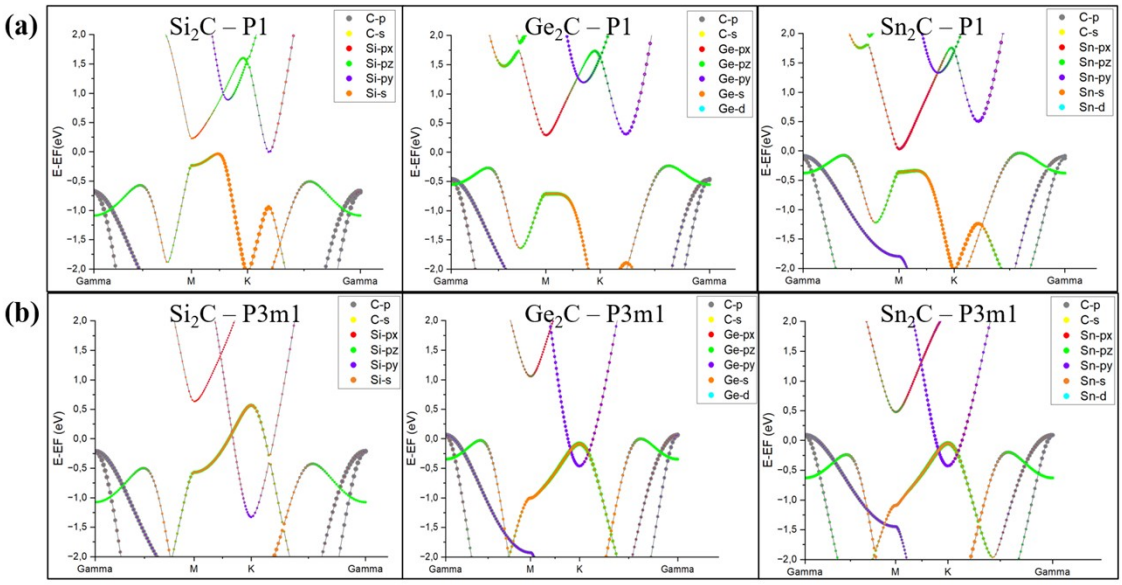

Figure S6. GGA-PBE band structures for the Si_2C, Ge_2C and Sn_2C monolayers in the P1 (a) and P3m1 (b) phases.

Table S1. Structural parameters for the optimized Si_2C monolayer at different phases. The C2/m, P1, and $P\bar{3}m1$ space group structures resemble the MXene Ti_2C one (Figure 1(a), right), while the structures of Cm, P3m1, and $P\bar{6}m2$ are similar to MoS_2 (Figure 1(a), left).

	C2/m	P1	$P\bar{3}m1$	Cm	P3m1	$P\bar{6}m2$
$d_{(X–X)}$ (Å)	2.8758	2.8772	2.8768	2.408	2.4085	2.4077
$d_{(X–C)}$ (Å)	2.0337	2.034	2.034	2.0435	2.0435	2.0437
C–X–C (°)	89.9747	89.9735	89.9895	88.7992	88.8012	88.8264
a (Å)	4.9806	2.8756	2.8762	4.9466	2.8595	2.8604
b (Å)	2.8754	2.8759	2.8762	2.8638	2.8595	2.8604
α (°)	90.0	90.6	90.0	90.0	90.0	90.0
β (°)	91.0387	93.9	90.0	90.0	90.0	90.0
γ (°)	90.0	120.0	120.0	90.0	120.0	120.0

Table S2. Structural parameters for the optimized Ge_2C monolayer at different phases. The C2/m, P1, and $P\bar{3}m1$ space group structures resemble the MXene Ti_2C one (Figure 1(a), right), while the structures of Cm, P3m1, and $P\bar{6}m2$ are similar to MoS_2 (Figure 1(a), left).

	C2/m	P1	$P\bar{3}m1$	Cm	P3m1	$P\bar{6}m2$
$d_{(X–X)}$ (Å)	3.0461	3.0417	3.0457	2.6058	2.5988	2.5962
$d_{(X–C)}$ (Å)	2.1844	2.1802	2.183	2.2133	2.2164	2.2156
C–X–C (°)	91.5899	91.5368	91.5297	88.8728	89.1089	89.1458
a (Å)	5.4244	3.1244	3.1281	5.3708	3.1099	3.1098
b (Å)	3.1318	3.1244	3.1281	3.1002	3.1099	3.1098
α (°)	90.0	90.7	90.0	90.0	90.0	90.0
β (°)	91.1041	94.2	90.0	90.0	90.0	90.0

γ (°)	90.0	120.0	120.0	90.0	120.0	120.0

Table S3. Structural parameters for the optimized Sn_2C monolayer at different phases. The C2/m, P1, and $P\bar{3}m1$ space group structures resemble the MXene Ti_2C one (Figure 1(a), right), while the structures of Cm, P3m1, and $P\bar{6}m2$ are similar to MoS_2 (Figure 1(a), left).

	C2/m	P1	$P\bar{3}m1$	Cm	P3m1	$P\bar{6}m2$
$d_{(X–X)}$ (Å)	3.3703	3.3684	3.3708	2.92	2.9193	2.918
$d_{(X–C)}$ (Å)	2.4008	2.3987	2.4003	2.4391	2.4399	2.4405
C–X–C (°)	90.839	90.805	90.7978	87.8871	87.889	87.9318
a (Å)	5.9236	3.416	3.4181	5.8625	3.3864	3.3885
b (Å)	3.4202	3.416	3.4181	3.3851	3.3864	3.3885
α (°)	90.0	91.0	90.0	90.0	90.0	90.0
β (°)	91.1246	89.9	90.0	90.0	90.0	90.0
γ (°)	90.0	120.0	120.0	90.0	120.0	120.0

Table S4. Differences in electronic dipole moments between two phases (Polar (P3m1) minus non-polar ($P\bar{6}m2$)) in Si_2C.

	Si_dn	Si_up	C
X	5.7e-05	-8e-06	6e-06
Y	-3.2e-05	4e-06	-4e-06
Z	-0.001755	3.6e-05	-0.000652

Table S5. Differences in electronic dipole moments between two phases (Polar (P3m1) minus non-polar ($P\bar{6}m2$)) in Ge_2C.

	Ge_dn	Ge_up	C
X	-2e-06	-4e-06	2e-06
Y	0.0	1e-06	-1e-06
Z	0.000183	-0.00074	0.000405

Table S6. Differences in electronic dipole moments between two phases (Polar (P3m1) minus non-polar ($P\bar{6}m2$)) in Sn_2C.

	Sn_dn	Sn_up	C
X	-6e-06	-3e-06	-6e-06
Y	3e-06	3e-06	4e-06
Z	-0.00249	-0.001844	-0.000866

Table S7. Differences in electronic dipole moments between two phases (Polar (P3m1) minus non-polar (P1)) in Si_2C.

	Si_dn	Si_up	C
X	-0.01385	0.013906	0.000466
Y	-0.010895	0.010937	-7.6e-05
Z	-0.064019	0.063903	-0.000228

Table S8. Differences in electronic dipole moments between two phases (Polar (P3m1) minus non-polar (P1)) in Ge_2C.

	Ge_dn	Ge_up	C
X	-0.015487	0.01513	-0.000132
Y	-0.012536	0.012278	-5.1e-05
Z	-0.053037	0.05245	0.000502

Table S9. Differences in electronic dipole moments between two phases (Polar (P3m1) minus non-polar (P1)) in Sn_2C.

	Sn_dn	Sn_up	C
X	-0.000189	-3.1e-05	-1.8e-05
Y	6e-05	-0.000177	5.2e-05
Z	-0.069498	0.066818	-0.000213

Table S10. Differences in electronic dipole moments between two phases (Polar (P3m1) minus non-polar (C2/m)) in Si_2C.

	Si_dn	Si_up	C
X	-3e-06	6e-06	-1e-05
Y	-4e-06	3e-06	6e-06
Z	-0.065012	0.064286	-0.000497

Table S11. Differences in electronic dipole moments between two phases (Polar (P3m1) minus non-polar (C2/m)) in Ge_2C.

	Ge_dn	Ge_up	C
X	0.000649	-0.000576	-1.2e-05
Y	-2.3e-05	-2.2e-05	7e-06
Z	-0.053864	0.053858	0.000346

Table S12. Differences in electronic dipole moments between two phases (Polar (P3m1) minus non-polar (C2/m)) in Sn_2C.

	Sn_dn	Sn_up	C
X	-0.000318	0.000389	-1.4e-05
Y	-2.2e-05	-1.8e-05	8e-06
Z	-0.068834	0.066626	8e-06

Table S13. Structural parameters, adsorption energies (E_{ads}) and binding energies (E_B) in heterostructures calculated with the DFT-D3 method.

	Si_2C(P3m1)	h-BN	Sn_2C(P1)	Sn_2C(P3m1)	NbS_2	Si_2C(P3m1)-h-BN	Sn_2C(P1)-NbS_2	Sn_2C(P3m1)-WSe_2

a (Å)	2.86	2.51	3.41	3.38	3.34	2.66	3.4	3.34
b (Å)	2.86	2.51	3.41	3.38	3.34	2.66	3.4	3.34
α (°)	90.0	90.0	91.04	90.0	90.0	90.16	90.19	90.0
β (°)	90.0	90.0	89.87	90.0	90.0	90.09	90.0	89.99
γ (°)	120.0	120.0	120.0	120.0	120.0	120.02	120.0	120.0
E_{ads} (eV)	-	-	-	-	-	0.73	-0.32	-0.12
E_B (eV)	-	-	-	-	-	-0.09	-0.35	-0.14